JOURNAL OF GUIDANCE, CONTROL, AND DYNAMICS
Vol. 30, No. 5, September–October 2007

Engineering Notes

ENGINEERING NOTES are short manuscripts describing new developments or important results of a preliminary nature. These Notes should not exceed 2500 words (where a figure or table counts as 200 words). Following informal review by the Editors, they may be published within a few months of the date of receipt. Style requirements are the same as for regular contributions (see inside back cover).

Optimal Formation Design for Imaging and Fuel Usage

Islam I. Hussein*
Worcester Polytechnic Institute, Worcester, Massachusetts 01609
Daniel J. Scheeres†
University of Michigan, Ann Arbor, Michigan 48109-2140
and
David C. Hyland‡
Texas A&M University, College Station, Texas 77843-3141

DOI: 10.2514/1.20080

I. Introduction

IN THIS paper we study optimal spacecraft formation motion design for fuel-image optimality. Previous results indicate a tradeoff between image quality and fuel expenditure [1,2]. Hence, we formulate an optimal control problem that optimizes fuel expenditure while meeting imaging goals. First, we state results from [3,4] that relate image quality to the trajectory of a sparse system of N telescopes. This relationship is used to define an optimal control problem that includes imaging and fuel performance measures. We then derive the necessary optimality conditions for a generic multispacecraft formation and specialize them to a two-spacecraft formation. We show that the optimal trajectory must be symmetric about the system center of mass, which in turn moves uniformly in space. We also show that there is a "speed control" effect that is necessary for meeting the desired image quality. Simulation results are provided to show the local behavior of the resulting control law. Finally, we prove optimality of a class of circular Earth-orbiting constellations introduced earlier in the literature [5]. This work is fundamental to current and future work related to motion path planning of deep-space, separated spacecraft interferometric missions used for the imaging of exosolar targets as those sought in NASA's Origins Program [6].

Presented as Paper 160 at the 2005 AAS/AIAA Space Flight Mechanics Meeting, Copper Mountain, CO, 23–27 January 2005; received 15 September 2005; revision received 6 September 2006; accepted for publication 8 September 2006.

*Assistant Professor, Mechanical Engineering, 100 Institute Road. AIAA Member.
†Associate Professor, Aerospace Engineering, 3048 FXB, 1320 Beal Avenue. AIAA Associate Fellow.
‡Professor, Aerospace Engineering and Director of Space Science and Space Engineering Research, 734 H. R. Bright Building.

II. Imaging Problem and Modulation Transfer Function

Refer to Fig. 1. Let σ denote an extended incoherent source. Let $\boldsymbol{q}' = (x_Q, y_Q, 0)$ and $\boldsymbol{q} = (x_P, y_P, z_P = \bar{z} + \zeta_P)$ be the positions of a point Q on the image plane I and a point P on the observation surface O'. The image plane I is the plane on which an image of σ is reconstructed and is set to be coincident with the x–y plane of our coordinate system, whose origin is at the geometric center of σ. On the other hand, the observation surface O' is one on which the constellation evolves and is located at a distance $\bar{z}$ from I. The observation plane is a plane through O' on which we project the motion of the constellation. Let D denote the effective dimension of the constellation, d denote the effective size of the target σ, and A_T denote the aperture area. There are two basic assumptions that we make in this paper. Firstly, the aperture area A_T of each craft is much smaller than the size of the constellation. In other words, $A_T \ll D^2$. Secondly, the observation plane O is assumed to be sufficiently far from the target σ. In other words, $D/\bar{z} \ll 1$ and $d/\bar{z} \ll 1$. The theory behind the model described next is applicable to any range of wavelengths, from infrared to radio-wave ranges [3]. Whereas in the infrared range metrology and control tolerances are very stringent, in radio-wave ranges tolerances are manageable with present day technology.

The main objective of the imaging constellation is to reconstruct the light intensity distribution deposited by σ on I using light collected in a set of regions $A_1, A_2, \ldots, A_N$, which represent the entry pupils of the separated telescopes and N is the number of apertures in the system. Under the assumptions that $A_T \ll D^2$, $D/\bar{z} \ll 1$, and $d/\bar{z} \ll 1$, one can show that the estimate of the image intensity $\hat{I}_e(\boldsymbol{\nu}) = \mathcal{F}[I_e(\boldsymbol{q})]$, where $\boldsymbol{\nu}$ is the spatial frequency and $\mathcal{F}$: $\mathbb{R}^2 \to \mathbb{R}^2$ is the Fourier transform, satisfies [3]

$$\hat{I}_e(\boldsymbol{\nu}, t) = \hat{M}(\boldsymbol{\nu}, t)\hat{I}(\boldsymbol{\nu}) \tag{1}$$

where $\hat{I}(\boldsymbol{\nu})$ is the true image intensity,

$$\hat{M}(\boldsymbol{\nu}, t) = \beta \sum_{m,n} \int_0^t \mathrm{d}\tau \hat{A}_p\left(\boldsymbol{\nu} - \frac{\boldsymbol{q}_{mn}(\tau)}{\lambda \bar{z}}\right) \tag{2}$$

β is a scalar constant, $\boldsymbol{q}_{mn}$ is the relative position between spacecraft m and n, λ is the wavelength, and $\hat{A}_p$ is the Fourier transform of the "field-of-view" or "picture frame" function

$$A_p(\boldsymbol{q}') = \begin{cases} 1 & \text{if } \boldsymbol{q}' \in I \\ 0 & \text{otherwise} \end{cases} \tag{3}$$

Note that the assumptions that $D/\bar{z} \ll 1$ and $d/\bar{z} \ll 1$ has directly led to the elimination of ζ_i from the derivation. Hence, Eq. (1) presents a valid model for the system whenever $\bar{z} \gg 1$. This assumption, however, does not imply that there is a need to constrain the formation to the observation plane O.

The function $\hat{M}$ is the modulation transfer function (MTF). Note that the MTF is simply the superposition of the functions $\hat{A}_p$, each evaluated at $\boldsymbol{q}_{mn}/(\lambda\bar{z})$. The MTF is defined as the ratio of the estimated intensity to the true image intensity. For an interferometric imaging constellation, the MTF can be computed given the measurement history and corresponding relative position data between the light collecting spacecraft. In the wave number plane, a

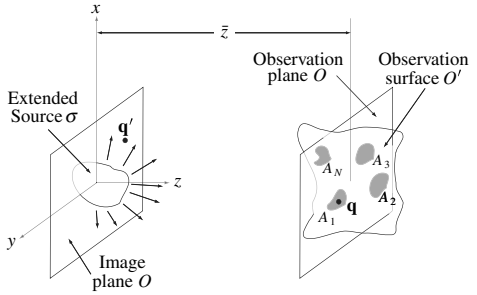

Fig. 1 Basic imaging situation.

point with a zero MTF value implies that the system is "blind" to the corresponding sinusoidal pattern, whereas a large value of the MTF implies that the image signal can be restored at that frequency. For more on the MTF, see [3,4] and references therein.

Let θ_r denote the desired angular resolution. The resolution disk D_v has a diameter $\simeq 1/\theta_r$ and is the region where we desire to have MTF > 0. We assume that

$$\hat{A}_p^2(\boldsymbol{\nu}) = \hat{A}_p(\boldsymbol{\nu}) = \begin{cases} 1 & \text{if } |\boldsymbol{\nu}| \le r_p \\ 0 & \text{otherwise} \end{cases} \tag{4}$$

where r_p is the effective radius of the true function $\hat{A}_p$. This model introduces a sensible error only at the edge of the domain of $\hat{A}_p$. This model is valid under the assumption that $D/\bar{z} \ll 1$ and $d/\bar{z} \ll 1$ [3,4]. The picture frame region is a circular disk of diameter $2r_p$ that is used to approximate the effective size of $\hat{A}_p$.

III. Multispacecraft Problem: Necessary Optimality Conditions

In this section, we derive the necessary optimality conditions for a multispacecraft formation by appealing to the maximum principle (MP). The dynamics are given by

$$\dot{\boldsymbol{q}}_i(t) = (t), \qquad \dot{\boldsymbol{v}}_i(t) = \boldsymbol{u}_i(t) \tag{5}$$

where $\boldsymbol{v}_i$ and $\boldsymbol{u}_i$ are the velocity and control vectors of spacecraft i. The cost function is

$$\mathcal{J} = y(T) = \int_0^T \mu\left(\sum_{i=1}^N \|\boldsymbol{u}_i(t)\|^2\right)\mathrm{d}t \tag{6}$$

where the cost $y(t)$ satisfies the differential equation

$$\dot{y}(t) = \mu \sum_{i=1}^N \|\boldsymbol{u}_i(t)\|^2 \tag{7}$$

In Eq. (7), μ is a parameter introduced to study the local behavior of the resulting control law in Sec. IV. An optimal solution will be independent of the parameter μ in general. Define the normalized MTF as

$$z(\boldsymbol{\nu}, t) = \frac{1}{\beta}\hat{M}(\boldsymbol{\nu}, t) - \int_0^t \sum_{n=1}^N \hat{A}_p(\boldsymbol{\nu} - \tilde{\boldsymbol{q}}_{nn})$$

The second term after the first equality sign in the definition of z ensures that z does not include contributions due to self-interaction at the origin of the frequency domain. Hence, for the spacecraft formation, z satisfies the differential equation

$$\dot{z}(\boldsymbol{\nu}, t) = \sum_m^N \sum_{n=1,\neq m}^N \hat{A}_p[\boldsymbol{\nu} - \tilde{\boldsymbol{q}}_{mn}(t)] \tag{8}$$

and is treated as a state of the system. Let $\tilde{\boldsymbol{q}}_{mn}$ denote the relative position vector between spacecraft m and n:

$$\tilde{\boldsymbol{q}}_{mn}(t) = (\boldsymbol{q}_m - \boldsymbol{q}_n)/(\lambda\bar{z}) \tag{9}$$

If we let h denote the saturation function $h(x) = x$ if $0 \le x < 1$ and $h(x) = 1$ if $x \ge 1$, then the terminal condition on z is given by

$$h[z(\boldsymbol{\nu}, T)] = 1 \tag{10}$$

for all $\boldsymbol{\nu} \in D_v$. This guarantees that $z \ge 1$ (i.e., complete coverage) everywhere inside D_v at time T. To summarize, initial and terminal conditions are

$$\begin{gathered} \boldsymbol{q}_i(0) = \boldsymbol{q}_{i0}, \qquad \boldsymbol{v}_i(0) = \boldsymbol{v}_i 0, \qquad y(0) = 0 \\ z(\boldsymbol{\nu}, 0) = 0, \quad \forall\ \boldsymbol{\nu} \in D_v, \qquad h[z(\boldsymbol{\nu}, T)] = 1, \quad \forall\ \boldsymbol{\nu} \in D_v \end{gathered} \tag{11}$$

The problem at hand is to minimize Eq. (6) subject to the dynamics of Eqs. (5), (7), and (8) and the boundary conditions in Eq. (11). We note that the system of Eqs. (5) and (8) involve three independent variables t and the two-dimensional spacial frequency $\boldsymbol{\nu} \in \mathbb{R}^2$. This kind of system resembles problems involving partial differential equations (PDEs) such as those in heat transfer and fluid mechanics (i.e., infinite-dimensional systems). There are two basic differences between our problem and infinite-dimensional problems such as the problem of controlling the temperature of a two-dimensional plate.

The first difference is that we do not have diffusion as evidenced by the absence of a partial differential equation in $\boldsymbol{\nu}$ governing z. In the PDE literature, this is known as an elliptic PDE. This is a special subclass of PDEs that also falls under the more general class of PDEs considered in, say, [7]. One novelty in this Note is that we identify the imaging problem as one that can be addressed using results from PDE systems theory. This potentially opens the door for using many of the results in control of PDE systems in the imaging problem.

The second difference is that in the plate temperature control problem we are able to control the temperature at each point on the plate. However, in our problem, the value of z can only be changed at frequencies where $\hat{A}_p$ has a nonzero value. In turn, the location of the $\hat{A}_p$ functions are determined by the dynamics governing $\boldsymbol{q}_i$.

In this Note, we use the MP to derive the necessary optimality conditions. We begin by defining the function

$$\begin{aligned} \hat{H}(t) = &\sum_{i=1}^N (\boldsymbol{p}_{\boldsymbol{q}_i} \cdot \boldsymbol{v}_i + \boldsymbol{p}_{\boldsymbol{v}_i} \cdot \boldsymbol{u}_i + \mu p_y \|\boldsymbol{u}_i\|^2) \\ &+ \left\langle p_z(\boldsymbol{\nu}, t), \sum_{m,n=1,n\neq m}^N \hat{A}_p(\boldsymbol{\nu} - \tilde{\boldsymbol{q}}_{mn}) \right\rangle \end{aligned} \tag{12}$$

where $\boldsymbol{p}_{\boldsymbol{q}_i}$ and $\boldsymbol{p}_{\boldsymbol{v}_i}$ are vector Lagrange multipliers, p_y is a scalar Lagrange multiplier, and p_z: $D_v \times [0, T] \to \mathbb{R}$ is a Lagrange multiplier function taken pointwise in $\boldsymbol{\nu}$. The inner product $\langle \cdot, \cdot \rangle$ in Eq. (12) is defined on the vector space of real functions whose domain is the resolution disk D_v: $\langle f(\boldsymbol{\nu}), g(\boldsymbol{\nu}) \rangle = \int_{D_v} f(\boldsymbol{\nu}) g(\boldsymbol{\nu})\, \mathrm{d}\boldsymbol{\nu}$, for any two functions f, g: $D_v \to \mathbb{R}$. A necessary condition for optimality is that $\partial \hat{H}/\partial \boldsymbol{u}_i = 0$, $i = 1, \ldots, N$. This implies that $\boldsymbol{u}_i = -\boldsymbol{p}_{\boldsymbol{v}_i}/2\mu p_y$, $i = 1, \ldots, N$. Hence, the Hamiltonian is given as

$$H(t) = \sum_{i=1}^N \left[\boldsymbol{p}_{\boldsymbol{q}_i} \cdot \boldsymbol{v}_i - \frac{\|\boldsymbol{p}_{\boldsymbol{v}_i}\|^2}{4\mu p_y}\right] + \left\langle p_z(\boldsymbol{\nu}, t), \sum_{m,n=1,n\neq m}^N \hat{A}_p(\boldsymbol{\nu} - \tilde{\boldsymbol{q}}_{mn}) \right\rangle \tag{13}$$

Transversality conditions imply [see Eq. (2.3.8) in [8]]

$$\boldsymbol{p}_{\boldsymbol{q}_i}(T) = \boldsymbol{p}_{\boldsymbol{v}_i}(T) = 0, \qquad p_z(\nu, T) = p_z^f(\boldsymbol{\nu}), \qquad p_y(T) = 1 \tag{14}$$

for some function p_z^f: $D_v \to \mathbb{R}$. By the MP, the necessary optimality conditions are given by

$$
\begin{aligned}
\dot{\boldsymbol{q}}_i(t) &= \frac{\partial H}{\partial \boldsymbol{p}_{\boldsymbol{v}_i}} = \boldsymbol{v}_i(t), \qquad \dot{\boldsymbol{v}}_i(t) = \frac{\partial H}{\partial \boldsymbol{p}_{\boldsymbol{v}_i}} = -\frac{\boldsymbol{p}_{\boldsymbol{v}_i}(t)}{2\mu p_y(t)} \\
\dot{y}_i(t) &= \frac{\partial H}{\partial p_y} = \sum_{i=1}^{N} \frac{\|\boldsymbol{p}_{\boldsymbol{v}_i}(t)\|^2}{4\mu p_y^2(t)} \\
\dot{z}(\boldsymbol{v},t) &= \frac{\partial H}{\partial p_z} = \sum_{m,n=1,n\neq m}^{N} \hat{A}_p[\boldsymbol{v} - \tilde{\boldsymbol{q}}_{mn}(t)] \\
\dot{\boldsymbol{p}}_{\boldsymbol{q}_i}(t) &= -\frac{\partial H}{\partial \boldsymbol{q}_i} = \frac{1}{\lambda\bar{z}}\left\langle p_z(\boldsymbol{v},t), \sum_{n=1,\neq i}^{N} -\nabla\hat{A}_p[\boldsymbol{v} - \tilde{\boldsymbol{q}}_{\text{in}}(t)] \right. \\
&\quad \left. + \nabla\hat{A}_p[\boldsymbol{v} + \tilde{\boldsymbol{q}}_{\text{in}}(t)]\right\rangle \\
\dot{\boldsymbol{p}}_{\boldsymbol{v}_i}(t) &= -\frac{\partial H}{\partial \boldsymbol{v}_i} = -\boldsymbol{p}_{\boldsymbol{q}_i}(t), \qquad \dot{p}_y(t) = -\frac{\partial H}{\partial y} = 0 \\
\dot{p}_z(\boldsymbol{v},t) &= -\frac{\partial H}{\partial z} = 0
\end{aligned}
\tag{15}
$$

From the initial and terminal conditions, the transversality conditions, Eq. (14), and the seventh and eighth equations in Eq. (15), we find that $p_y(t) = 1$ and $p_z(\boldsymbol{v},t) = p_z^f(\boldsymbol{v})$ for all $t \in [0,T]$. We have

$$
\begin{aligned}
&\dot{\boldsymbol{q}}_i(t) = \boldsymbol{v}_i(t), \quad \dot{\boldsymbol{v}}_i(t) = -\frac{\boldsymbol{p}_{\boldsymbol{v}_i}(t)}{2\mu}, \quad \dot{y}_i(t) = \sum_{i=1}^{N} \frac{\|\boldsymbol{p}_{\boldsymbol{v}_i}(t)\|^2}{4\mu} \\
&\dot{z}(\boldsymbol{v},t) = \sum_{m,n=1}^{N} \hat{A}_p[\boldsymbol{v} - \tilde{\boldsymbol{q}}_{mn}(t)] \\
&\dot{\boldsymbol{p}}_{\boldsymbol{q}_i}(t) = \frac{1}{\lambda\bar{z}}\left\langle p_z^f(\boldsymbol{v}), \sum_{n=1,\neq i}^{N} -\nabla\hat{A}_p[\boldsymbol{v} - \tilde{\boldsymbol{q}}_{\text{in}}(t)] + \nabla\hat{A}_p[\boldsymbol{v} + \tilde{\boldsymbol{q}}_{\text{in}}(t)]\right\rangle \\
&\dot{\boldsymbol{p}}_{\boldsymbol{v}_i}(t) = -\boldsymbol{p}_{\boldsymbol{q}_i}(t)
\end{aligned}
\tag{16}
$$

IV. Two-Spacecraft Problem

In this section, we derive the necessary conditions for a two-spacecraft formation using the MP. Because we have two degrees of freedom, instead of using the positions of the spacecraft as system states, we will use the relative position between the spacecraft and the position of the center of mass as our states. As before, let $\tilde{\boldsymbol{q}}$ denote the relative position vector between the spacecraft pair divided by $\lambda\bar{z}$

$$
\tilde{\boldsymbol{q}}(t) = [\boldsymbol{q}_2(t) - \boldsymbol{q}_1(t)]/(\lambda\bar{z}) \tag{17}
$$

where $\boldsymbol{q}_i$, $i = 1, 2$, is the position vector of the two spacecraft. $\tilde{\boldsymbol{q}}$ corresponds to the motion of one of the picture frame disks in the frequency domain. Let $\mathbf{s}$ be the position vector of the center of mass of the formation

$$
\boldsymbol{s}(t) = [\boldsymbol{q}_2(t) + \boldsymbol{q}_1(t)]/2 \tag{18}
$$

where we assume unity mass for both spacecraft. The dynamics of the system are given by

$$
\begin{aligned}
\dot{\tilde{\boldsymbol{q}}}(t) = \boldsymbol{v}_{\boldsymbol{q}}(t), \quad \dot{\boldsymbol{v}}_{\boldsymbol{q}}(t) = [\boldsymbol{u}_2(t) - \boldsymbol{u}_1(t)]/(\lambda\bar{z}), \quad \dot{\boldsymbol{s}}(t) = \boldsymbol{v}_{\boldsymbol{s}}(t) \\
\dot{\boldsymbol{v}}_{\boldsymbol{s}}(t) = [\boldsymbol{u}_2(t) + \boldsymbol{u}_1(t)]/2
\end{aligned}
\tag{19}
$$

The cost function to be minimized is given by Eqs. (6) and (7), subject to Eqs. (7) and (8) with $N = 2$, Eq. (19), and initial and terminal conditions are

$$
\tilde{\boldsymbol{q}}(0) = \tilde{\boldsymbol{q}}_0, \quad \boldsymbol{v}_{\boldsymbol{q}}(0) = \boldsymbol{v}_{\boldsymbol{q}_0}, \quad \boldsymbol{s}(0) = \boldsymbol{s}_0, \quad \boldsymbol{v}_{\boldsymbol{s}}(0) = \boldsymbol{v}_{\boldsymbol{s}_0}, \quad y(0) = 0 \tag{20}
$$

Again, we use the MP to derive the necessary conditions. Hence, we have

$$
\begin{aligned}
\hat{H}(t) =& \boldsymbol{p}_{\boldsymbol{q}}(t)\cdot\boldsymbol{v}_{\boldsymbol{q}}(t) + \tfrac{1}{\lambda\bar{z}}\boldsymbol{p}_{v_q}(t)\cdot[\boldsymbol{u}_2(t) - \boldsymbol{u}_1(t)] + \boldsymbol{p}_s(t)\cdot\boldsymbol{v}_{\boldsymbol{s}}(t) \\
&+ \frac{1}{2}\boldsymbol{p}_{v_s}(t)\cdot[\boldsymbol{u}_1(t) + \boldsymbol{u}_2(t)] + \mu p_y(t)[\|\boldsymbol{u}_1(t)\|^2 + \|\boldsymbol{u}_2(t)\|^2] \\
&+ \langle p_z(\boldsymbol{v},t), \hat{A}_p[\boldsymbol{v} - \tilde{\boldsymbol{q}}(t)] + \hat{A}_p(\boldsymbol{v} + \tilde{\boldsymbol{q}})\rangle
\end{aligned}
\tag{21}
$$

where $\boldsymbol{p}_{\boldsymbol{q}}$, $\boldsymbol{p}_{v_q}$, $\boldsymbol{p}_s$, and $\boldsymbol{p}_{v_s}$ are vector Lagrange multipliers, p_y is a scalar Lagrange multiplier, and p_z: $D_v \times [0,T] \to \mathbb{R}$ is a Lagrange multiplier function taken pointwise in $\boldsymbol{v}$. A necessary condition for optimality is that $\partial\hat{H}/\partial\boldsymbol{u}_1 = \partial\hat{H}/\partial\boldsymbol{u}_2 = 0$. These imply that

$$
\begin{aligned}
\boldsymbol{u}_1(t) &= \frac{1}{2\mu p_y(t)}\left[\frac{\boldsymbol{p}_{v_q}(t)}{\lambda\bar{z}} - \frac{\boldsymbol{p}_{v_s}(t)}{2}\right] \\
\boldsymbol{u}_2(t) &= -\frac{1}{2\mu p_y(t)}\left[\frac{\boldsymbol{p}_{v_q}(t)}{\lambda\bar{z}} + \frac{\boldsymbol{p}_{v_s}(t)}{2}\right]
\end{aligned}
$$

Transversality conditions give

$$
\begin{aligned}
\boldsymbol{p}_{\boldsymbol{q}}(T) = \boldsymbol{p}_{v_q}(T) = \boldsymbol{p}_s(T) = \boldsymbol{p}_{v_s}(T) = 0, \quad p_z(\boldsymbol{v},T) = p_z^f(\boldsymbol{v}) \\
p_y(T) = 1
\end{aligned}
\tag{22}
$$

After applying terminal and transversality conditions, the necessary conditions are found to be $\boldsymbol{p}_s(t) = \boldsymbol{p}_{v_s} = 0$, $\boldsymbol{s}(t) = \boldsymbol{s}_0$, and $\boldsymbol{v}_{\boldsymbol{s}} = \boldsymbol{v}_{\boldsymbol{s}_0}$ for all $t \in [0,T]$. This implies that $\boldsymbol{u}_1 = -\boldsymbol{u}_2$. Hence, a necessary optimality condition is that the center of mass drifts with constant velocity. That is because, firstly, motion of the center of mass does not affect image quality. Secondly, an accelerated motion of the center of mass will result in additional unnecessary fuel expenditure. And so, it is intuitive that the center of mass be fixed as an optimality necessary condition.

Finally, after omitting equations related to the motion of the center of mass, the preceding discussion implies that the necessary conditions are

$$
\begin{aligned}
&\dot{\tilde{\boldsymbol{q}}}(t) = \boldsymbol{v}_{\boldsymbol{q}}(t), \qquad \dot{\boldsymbol{v}}_{\boldsymbol{q}}(t) = -\frac{\boldsymbol{p}_{v_q}(t)}{\mu(\lambda\bar{z})^2}, \qquad \dot{y}(t) = \frac{\|\boldsymbol{p}_{v_q}(t)\|^2}{2\mu(\lambda\bar{z})^2} \\
&\dot{z}(\boldsymbol{v},t) = \hat{A}_p[\boldsymbol{v} - \tilde{\boldsymbol{q}}(t)] + \hat{A}_p[\boldsymbol{v} + \tilde{\boldsymbol{q}}(t)] \\
&\dot{\boldsymbol{p}}_{\boldsymbol{q}}(t) = -\langle p_z^f(\boldsymbol{v}), -\nabla\hat{A}_p[\boldsymbol{v} - \tilde{\boldsymbol{q}}(t)] + \nabla\hat{A}_p[\boldsymbol{v} + \tilde{\boldsymbol{q}}(t)]\rangle \\
&\dot{\boldsymbol{p}}_{v_q}(t) = -\boldsymbol{p}_{\boldsymbol{q}}(t)
\end{aligned}
\tag{23}
$$

These equations are the necessary optimal conditions for the two-craft problem. These and the transversality conditions in Eq. (22) represent a two-point boundary value problem. Although not sufficient, these conditions are helpful in that one can study the general behavior of an optimal solution. We may also numerically investigate whether the previously given control law behaves as we would expect it to. We will treat the problem as an initial value problem by selecting arbitrary initial values for the adjoint variables. Note here that our goal is not to solve for the extremals of the optimal control problem. We merely desire to study the dynamic behavior of trajectories that flow according to the conditions in Eq. (23). We perform the simulation using Matlab. D_v is such that it is 30 pixels in diameter. The picture frame disk is 4 pixels in diameter. We use the Matlab function "gradient" to compute the gradient of the picture frame functions. We normalize the position vector $\bar{q}$ such that position is given in terms of number of pixels and $\bar{v}_q$ in terms of pixels per second. The duration of the simulation is 50 sec and $\lambda\bar{z} = 1 \times 10^4$. We also set $\mathbf{p_q}(0) = (0,0)$, $\mathbf{p}_{v_q}(0) = (0,0)$, and $p_z^f(\boldsymbol{v})$, $\forall\ \boldsymbol{v} = -1000$. We use these values for all simulations. We consider four numerical examples. The parameters are set as shown in Table 1.

In Figure 2a, we investigate the behavior of the picture frame disk when it gets a "head-on" impact with the boundary of the resolution disk. The behavior shown agrees with our intuition behind the formulation of the optimal control problem in that the picture frame disks move in directions seeking to achieve $z(\boldsymbol{v},T) \geq 1$ to satisfy the

Table 1 Variable choices for numerical examples

Example in	$\bar{q}_0$	$\bar{v}_0$	μ
Fig. 2a	(9, 9)	(−1, 1)	1×10^{-6}
Fig. 2b	(13, 2)	(−10, 0)	1×10^{-6}
Fig. 2c	(13, 2)	(−9, 0)	1×10^{-4}

terminal condition. We note that the trajectory is very sensitive to our choice of $p_z^f(\boldsymbol{\nu})$.

Another interesting behavior is given in Figs. 2b and 2c. In these two examples we investigate the response of the control law to the speed of the picture frame disks. How the value of $z(\boldsymbol{\nu}, t)$ is related to speed of motion is discussed in [3] and Sec. V.A. In Figure 2, the initial velocity is set too large and we note that coverage improves as the picture frame disks move (this is observed by the fact that coverage becomes darker in color). The initial speed in Fig. 2b is larger than that in Fig. 2c. We note that, in the former case, coverage converges to a darker shade of red less rapidly than that in the latter case. This is true assuming that we have chosen a value for $p_z^f(\boldsymbol{\nu})$ that is close enough to the desired value.

V. Particular Solutions

A. Two-Spacecraft, One-Dimensional Problem

In this section, we further specialize Eqs. (23) to the two-spacecraft, one-dimensional case. By one-dimensional, we mean that the wave number resolution disk D_v collapses to a wave number interval $\mathcal{L}_v = [-L_v/2, L_v/2]$, where $L_v/2$ is the bound on the frequency content of the signal to be reconstructed (that is, L_v is the width of the resolution interval).

This one-dimensional problem is analogous to the spiraling, one-dimensional problem studied in [3,4]. However, the simple linear example has an important theoretical implication because, locally in time, the motion of any particular picture frame disk in the two-dimensional case can be approximated by a one-dimensional linear motion. Hence, studying the one-dimensional case gives insight into the local-time behavior of the picture frame disk. For example, studying how a one-dimensional picture frame disk interacts with partially covered ($z < 1$) one-dimensional intervals along the line of motion enables us to understand how a two-dimensional picture frame disk infinitesimally interacts with neighboring (two-dimensional) coverage areas.

In the one-dimensional case, the necessary conditions become

$$\dot{q} = v, \qquad \dot{v} = -p_v/[\mu(\lambda\bar{z})^2], \qquad \dot{y} = \|p_v\|^2/[2\mu(\lambda\bar{z})^2]$$
$$\dot{z}(\nu, t) = \hat{A}_p(\nu - q) + \hat{A}_p(\nu + q)$$
$$\dot{p}_q = -\left\langle p_z^f(\nu), -\frac{\mathrm{d}}{\mathrm{d}\nu}\hat{A}_p(\nu - q) + \frac{\mathrm{d}}{\mathrm{d}\nu}\hat{A}_p(\nu + q)\right\rangle, \qquad \dot{p}_v = -p_q \tag{24}$$

where we omit the subscript q in v_q and remove the over-bars that indicated vector-valued variables. The inner product $\langle \cdot, \cdot \rangle$ refers to the inner product on the vector space of real functions whose domain is the resolution interval

$$\mathcal{L}_v\colon \langle f(\nu), g(\nu)\rangle = \int_{-L_v/2}^{L_v/2} f(\nu)g(\nu)\,\mathrm{d}\nu$$

for any two functions $f, g\colon \mathcal{L}_v \to \mathbb{R}$. The initial and terminal conditions are given by

$$q(0) = q_0, \qquad v(0) = v_0, \qquad y(0) = 0, \qquad z(\nu, 0) = 0$$
$$z(\nu, T) = 1, \qquad p_q(T) = 0, \qquad p_v(T) = 0$$

Note also that the gradient operator changes to a simple derivative over the frequency domain. Under the model given in Eq. (4), we then have

$$\hat{A}_p(\nu - q) = \begin{cases} 1 & q - r_p \le \nu \le r_p + q \\ 0 & \text{otherwise} \end{cases} \quad \text{and}$$
$$\hat{A}_p(\nu + q) = \begin{cases} 1 & -r_p - q \le \nu \le r_p - q \\ 0 & \text{otherwise} \end{cases}$$

and, hence

$$\frac{\mathrm{d}}{\mathrm{d}\nu}\hat{A}_p(\nu - q) = \delta[\nu - (q - r_p)] - \delta[\nu - (q + r_p)]$$
$$\frac{\mathrm{d}}{\mathrm{d}\nu}\hat{A}_p(\nu + q) = \delta[\nu - (-r_p - q)] - \delta[\nu - (r_p - q)]$$

where $\delta(x)$ is the Dirac delta function (assuming the picture frame function $\hat{A}_p$ assumes a Heaviside step function).

We study a trajectory such that the picture frame disks move with a constant critical speed v_c

$$q(t) = -v_c t + q_0 \tag{25}$$

We choose $q_0 = (L_v/2) + r_p$ such that the picture frame disks are initially located right outside the resolution interval. The critical speed v_c is the speed that guarantees that at any frequency component $\nu \in [-L_v/2, L_v/2]$ we achieve $z(\nu, T) = 1$ at the end of the maneuver with only a single passage over the resolution interval. Note that $z(\nu, t)$ is equal to the amount of time spent by the frequency ν inside one of the picture frame disks up to time t. These choices imply that we have to set $v_c = 2r_p$ to ensure that $z = 1$ at each frequency inside the resolution interval $[-L_v/2, L_v/2]$. The terminal time T is chosen such that $q(T) = 0$. Hence, we have $T = 1/2 + (L_v/2)/v_c$. We will fix this terminal time value and assume it is chosen as such beforehand.

Equation (25) and the necessary conditions in Eq. (24) imply that $v(t) = -v_c$, $p_q(t) = 0$, $p_v(t) = 0$, $p_z(\nu, t) = p_z^f(\nu)$. Thus, we are left with

$$\dot{y} = 0, \qquad \dot{z}(\nu, t) = \hat{A}_p(\nu - q) + \hat{A}_p(\nu + q)$$
$$0 = p_z^f(\nu = q - r_p, t) - p_z^f(\nu = q + r_p, t) + p_z^f(\nu = -q - r_p, t)$$
$$- p_z^f(\nu = -q + r_p, t) \tag{26}$$

$\forall\ t \in [0, T]$. The first of these equations and the initial condition $y(0) = 0$ implies that $y(t) = 0$ for all $t \in [0, T]$. In particular, we have $y(T) = 0$. Hence, the proposed solution achieves zero cost. Because the cost functional $\mathcal{J}$ is positive definite, then any solution that

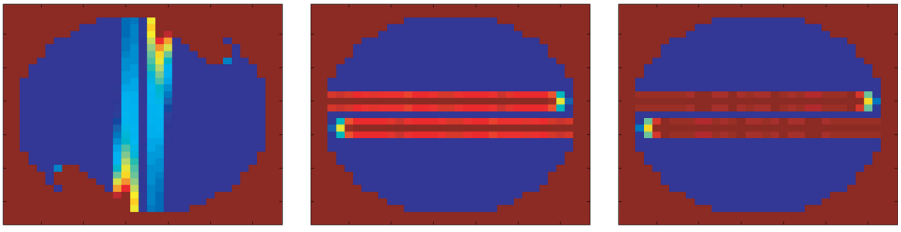

Fig. 2 Motion of the picture frame disks in the u–v plane at a) $t = 10$ s, b) $t = 3$ s, and c) $t = 3.5$ s for three different initial conditions (see Table 1).

achieves zero cost and satisfies the terminal condition is then an optimal solution.

In [9], the authors show that the terminal conditions are satisfied for the proposed motion. By construction, the time spent by the picture frame disk over ν turns out to be exactly equal to one [9]. Because we do not have double passages over any frequency point ν, then at $t = T$, $z(\nu, T) = 1$, for all $\nu \in \mathcal{L}_v$. This shows that the proposed motion is indeed optimal because it achieves zero cost and satisfies the desired terminal conditions. To complete the proof, we just need to show that the third condition in Eqs. (26) is satisfied for all $t \in [0, T]$. Note that the function $p_z^f(\nu)$ does not influence the remaining necessary conditions. Hence, any choice for $p_z^f(\nu)$ that will set the right-hand side equal to zero is a valid choice. For instance, any symmetric function $p_z^f(\nu)$ will satisfy this condition because the second term in the inner product is skew symmetric (if f is symmetric and g is skew symmetric, then $\langle f, g \rangle = 0$). Indeed, $p_z^f(\nu) \equiv 0$ for all $\nu \in \mathcal{L}_v$ is a valid choice.

B. Class of Circular Earth-Orbiting Observatories

In this section, we show that a circular Earth-orbiting observatory that was introduced in [5] is optimal. This class of constellations is designed to achieve complete wave number plane coverage. This constellation was further studied in [10] to examine the effect of orbit perturbations on the quality of the reconstructed image and to examine ways to correct the design to counteract these perturbations. The satellite constellation is placed on a circular arc that is a segment of an Earth orbit and whose center is located at the center of the Earth (see Fig. 3). The basic assumption is that the formation maintains its rigidity. The Earth-orbiting observatory will maintain formation even when in eccentric orbits as long as the spacecraft elliptic motions are in phase and have the same value for the semimajor axis. The satellites are distributed such that the second satellite is located at a distance of $d_{\min}$ from the first satellite, the third at $2d_{\min}$ from the first, the fourth at $3d_{\min}$ from the first, and so on. This arrangement ensures the complete coverage of the wave number plane once every half an orbit period [5]. Figure 3 shows the geometry of this configuration for $N_f = 3$ satellites. We nominally assume that the orbit plane is perpendicular to the line of sight to the target. The motion in the frequency domain is as shown in Figure 3.

We choose the terminal time T such that T spans an integer multiple, say l, of the orbit period T_o: $T = lT_o$. The reason for having to wait for multiple orbits before capturing an image is due to the fact that coverage in the frequency domain is radially uneven. That is to say, for each $\nu^* \in \mathbb{R}$, we have even coverage for all $\boldsymbol{\nu}$ satisfying $\|\boldsymbol{\nu}\| = \nu^*$ after each half orbit period. However, as ν^* changes, the value of z changes (in fact, decreases as shown earlier). Hence, we choose l such that after $l/2$ orbit periods the value of $z(\boldsymbol{\nu}, t)$ is at least unity everywhere inside the resolution disk D_v. Specifying T automatically specifies the orbit size.

A similar analysis as before gives the following necessary conditions

$$\begin{aligned} &\dot{\boldsymbol{q}}_i(t) = \boldsymbol{v}_i(t), \qquad \dot{\boldsymbol{v}}_i(t) = \boldsymbol{g}(\boldsymbol{q}_i), \qquad \dot{y}(t) = 0 \\ &\dot{z}(\boldsymbol{\nu}, t) = \sum_{l,n=1,n\neq l}^{N} \hat{A}_p[\boldsymbol{\nu} - \boldsymbol{q}_{mn}(t)] \\ &0 = \left\langle p_z^f(\boldsymbol{\nu}), \sum_{n=1,\neq i}^{N} -\nabla\hat{A}_p(\boldsymbol{\nu} - \boldsymbol{q}_{\text{in}}) + \nabla\hat{A}_p(\boldsymbol{\nu} + \boldsymbol{q}_{\text{in}}) \right\rangle \end{aligned} \tag{27}$$

where $\boldsymbol{g}$ is the central gravitational force.

Note that the first two equations in Eqs. (27) simply express the Keplerian motion in differential equation form, which is necessary by design. Secondly, the initial condition $y(0) = 0$ and the third equation gives $y(t) = 0$ for all $t \in [0, T]$. In particular, the total cost is $y(T) = 0$. Because the cost functional is positive definite, then if the formation satisfies the terminal necessary conditions, then the Earth-orbiting observatory *is optimal*. To check for this, we need to verify that the terminal condition in Eq. (10) and that the last condition in Eq. (27) are satisfied. By construction, the formation makes enough orbits l such that at terminal time T we have $h[z(\boldsymbol{\nu}, T)] = 1$ and, hence, satisfying the terminal condition. Similar to the discussion made in the last paragraph of Sec. V.A, any symmetric function $p_z^f(\boldsymbol{\nu})$ [such as $p_z^f(\boldsymbol{\nu}) \equiv 0$] will satisfy this condition by symmetry of the second term in the inner product. This shows that the Earth-orbiting formation is an optimal solution to the problem.

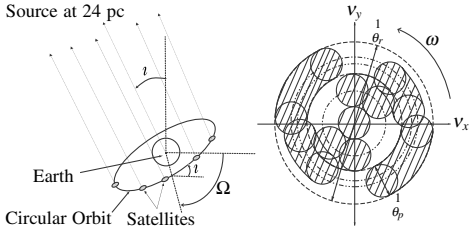

Fig. 3 Wave number plane coverage for a three-spacecraft formation.

Finally, note that in [10], the authors propose thrust-free designs that guarantee full coverage of the frequency domain for the circular orbit observatory under general (and, in particular, J_2) perturbations. Although the craft may not be rigidly moving together, zero-thrust solutions that meet the imaging requirements do exist and the result presented in this section applies to the case in which perturbations are present after nominal design modifications as proposed in [10].

VI. Conclusions

In this Note, we study an optimal control problem for optimal image and fuel usage. The main contribution of this Note is to show that an optimal trajectory must be symmetric about the origin. We also show that an optimal trajectory has a "speed control" property that is desirable for uniform coverage of the u–v space. This is shown to be true using numerical simulations. Finally, we show that a class of Earth-orbiting constellations introduced earlier in the literature is optimal. Future research will focus on the mathematical formalism of optimal control of infinite-dimensional systems with and without diffusion, with special focus on the latter case. We will also seek to find solutions to the N-spacecraft problem other than the Earth-orbiting constellation.

References

[1] Hussein, I. I., Scheeres, D. J., and Hyland, D. C., "Control of a Satellite Formation for Imaging Applications," *Proceedings of the 2003 American Control Conference*, Inst. of Electrical and Electronics Engineers, New York, June 2003, pp. 308–313.

[2] Hussein, I. I., Bloch, A. M., Scheeres, D. J., and McClamroch, N. H., "Optimal Fuel-Image Motion Planning for a Class of Dual Spacecraft Formations," *2005 American Control Conference*, Inst. of Electrical and Electronics Engineers, New York, 2005, pp. 2405–2410.

[3] Hussein, I. I., "Motion Planning for Multi-Spacecraft Interferometric Imaging Systems," Ph.D. Dissertation, Univ. of Michigan, Ann Arbor, MI, 2005.

[4] Chakravorty, S., "Design and Optimal Control of Multi-Spacecraft Interferometric Imaging Systems," Ph.D. Dissertation, Aerospace Engineering, Univ. of Michigan, Ann Arbor, MI, 2004.

[5] Hussein, I. I., Scheeres, D. J., and Hyland, D. C., "Interferometric Observatories in Earth Orbit," *Journal of Guidance, Control, and Dynamics*, Vol. 27, No. 2, 2004, pp. 297–301.

[6] "NASA Origins Program," http://origins.jpl.nasa.gov [retrieved 2004].

[7] Lions, J. L., *Optimal Control of Systems Governed by Partial Differential Equations*, Springer–Verlag, Berlin, 1971.

[8] Bryson, A. E., and Ho, Y., *Applied Optimal Control*, Hemisphere, New York, 1975.

[9] Hussein, I. I., Scheeres, D. J., and Hyland, D. C., "Optimal Formation Control for Imaging and Fuel Usage with Terminal Imaging Constraints," *2005 IEEE Conference on Control Applications*, Inst. of Electrical and Electronics Engineers, New York, 2005, pp. 352–357.

[10] Hussein, I. I., and Scheeres, D. J., "Effects of Orbit Variations and J_2 Perturbations on a Class of Earth-Orbiting Interferometric Observatories," *Journal of the Astronautical Sciences*, Vol. 53, No. 2, 2005.